High-performance aromatic polyimide fibres: 2. Thermal mechanical and dynamic properties

Mark Eashoo, Dexing Shen, Zongquan Wu, Chul Joo Lee, Frank W. Harris and Stephen Z. D. Cheng*

Institute and Department of Polymer Science, College of Polymer Science and Polymer Engineering, The University of Akron, Akron, OH 44325-3909, USA

(Received 28 September 1992; revised 13 November 1992)

A family of high-temperature, high-modulus aromatic polyimide fibres has been dry-jet wet spun from either its gel state or isotropic solution, followed by high-temperature drawing. In this report, thermal and dynamic mechanical properties of one of the family members, a segmented rigid-rod polyimide synthesized from 3,3',4,4'-biphenyltetracarboxylic dianhydride (BPDA) and 2,2'-bis(trifluoromethyl)-4,4'-diaminobiphenyl (PFMB), are presented in detail. Mechanical properties of these BPDA–PFMB fibres can be improved remarkably by drawing due to drastic increases in overall orientation, crystal orientation and crystallinity. These three structural parameters, however, do not show parallel changes with increasing draw ratio. It has been observed that the linear coefficient of thermal expansion (CTE) of BPDA–PFMB fibres after drawing generally show negative values in the solid state when low stresses are applied during measurements. For as-spun fibres, the CTEs are constant over a certain applied stress region, which is on the same order of magnitude as CTEs of in-plane oriented BPDA–PFMB films along the film surface. This may be an indication that within this region the stress applied is at the same level as the internal stress frozen into the fibres during spinning and drawing. Glass transition temperatures (T_g) of as-spun fibres show a linear decrease at low applied stress region, then level off when the applied stress becomes high. Dynamic mechanical data indicate two relaxation processes in as-spun fibres above room temperature: an α relaxation corresponding to the glass transition and a β relaxation which is a subglass transition. In the fibres with a draw ratio of above three times, the α relaxation is totally suppressed. This reveals a rigid fraction (above T_g) dependence of this relaxation in the fibres. The β relaxation is, on the other hand, crystallinity dependent. The Arrhenius activation energy (about 160 kJ mol^{-1}) of the β relaxation in as-spun fibres is about 50 kJ mol^{-1} lower than that of drawn fibres, indicating that the cooperativity of molecular motion in the fibre changes with orientation and crystallinity.

(Keywords: aromatic polyimide; BPDA–PFMB fibres; coefficient of thermal expansion; cooperativity; crystal orientation; crystallinity; dynamic mechanical property; modulus; molecular motion; overall orientation; subglass transition; tensile strength; thermal mechanical property)

INTRODUCTION

In the first part of this series[1] we reported a new high-performance aromatic polyimide fibre. The polymer was synthesized from 3,3',4,4'-biphenyltetracarboxylic dianhydride (BPDA) and 2,2'-bis(trifluoromethyl)-4,4'-diaminobiphenyl (PFMB) in refluxing *m*-cresol at elevated temperatures. Therefore poly(amic acid) precursors were not isolated[2,3]. This polyimide is soluble in *m*-cresol and other hot phenolic solvents in concentrations of up to 15(w/w)% or even higher. An isotropic solution can be observed during the polymerization at 10(w/w)%. Upon cooling, the solution sets becoming a gel with mechanical strength. This mechanical gel state is thermally reversible to become the sol during heating. At lower temperatures, an anisotropic ordered state starts developing, evidenced by polarized light microscopy, differential scanning calorimetry and small-angle light scattering[4]. Based on the phase boundaries of both mechanical gel/sol and anisotropic order/disorder transitions, it is found that there is a temperature region in which the anisotropic ordered state has no longer existed, but the mechanical gel remains. For example, a solution concentration of 10(w/w)% with an intrinsic viscosity of 5.0 shows a temperature region of about 10°C[4]. This region actually serves as a processing window for fibre spinning.

The fibres are spun via dry-jet wet spinning from the BPDA–PFMB gel or isotropic liquid state. As-spun fibres are quenched in a coagulation bath of water and methanol. Extensive drawing is performed at elevated temperatures to increase the fibres' mechanical properties. The highly drawn fibres with a draw ratio of eight to ten show tensile properties[1] with a strength of 3.2 GPa and a modulus of 130 GPa. BPDA–PFMB fibres also show excellent thermal stability and retain relatively high tensile strength and modulus at elevated temperatures. Highly drawn BPDA–PFMB fibres display a distinct wide-angle X-ray diffraction (WAXD) pattern, from which a monoclinic unit cell has been determined[1,5].

* To whom correspondence should be addressed

0032-3861/93/153209-07

Furthermore, changes in crystallographic parameters such as apparent crystallite sizes, degree of crystallinity and crystal orientation have been related to different draw ratios in the fibres[1].

In this publication, as the second paper in this series, we concentrate on the detailed development of overall orientation and crystal orientation for various draw ratios observed through optical birefringence (o.b.) and WAXD methods. A study of thermal mechanical (TM) and dynamic mechanical (DM) properties of single BPDA–PFMB filaments is also carried out. Glass transition temperature (T_g) and linear coefficients of thermal expansion (CTE) along the fibre direction at different draw ratios are investigated. The dynamic mechanical (DM) properties of the single filaments provide experimental evidence of changes in the relaxation processes with different draw ratios. These properties are, in turn, correlated with structural parameter changes, in particular, fibre orientations and crystallinity.

EXPERIMENTAL

Materials and fibre spinning

BPDA–PFMB was polymerized from an aromatic dianhydride (BPDA) and a diamine (PFMB) in hot *m*-cresol at a solid content of about 10(w/w)%. The condensation reaction was carried out at about 180°C in refluxing solvent. No poly(amic acids) were isolated[2,3]. The intrinsic viscosity of the BPDA–PFMB in *m*-cresol at 60°C was 5.5 dl g^{-1}. The chemical structure of BPDA–PFMB is

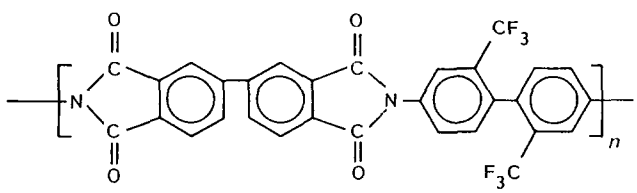

The polymer solution was degassed at 100°C after polymerization. Fibre spinning was conducted on a dry-jet wet spinning machine which was home-designed in our laboratory. It includes a spinning head, spinneret with an adjustable dry-jet path, coagulation bath and winder. The fibres were spun from either the gel state or an isotropic solution. It has been found that fibres spun from the gel state provide relatively better initial as-spun fibre properties. Different draw ratios were prepared by a zone-drawing method between 300°C and 420°C at a constant force of 0.002 N in air. As-spun fibres can be drawn as high as ten times.

Equipment and experiments

Overall orientation in the BPDA–PFMB fibres with different draw ratios was determined by the optical birefringence (o.b.) method. A 20-order tilting compensator (Liez) was coupled with an Olympus polarized light microscope (PLM). The birefringences of the fibres were measured following the standard procedure[6].

WAXD experiments were performed on a 12 kW Rigaku rotating anode X-ray generator and a vacuum camera. The wavelength of Cu-K_α X-ray incident beam is 0.154 nm. Diffraction patterns of the fibres with different draw ratios were taken, and the crystal orientation along certain crystallographic planes was calculated using Hermann's equation of

$$f_c(003) = (3\langle\cos^2 \Phi_c\rangle - 1)/2 \quad (1)$$

where f_c is the orientation factor along the fibre direction and Φ_c represents the angle between the fibre direction and the c-axis of the crystal unit cell. The numerical values of the mean-square cosines in equation (1) can be determined from the fully corrected intensity distribution diffracted from (003) crystallographic plane, $I_c(\Phi_c, \alpha)$, averaged over the entire surface of the orientation sphere:

$$\langle\cos^2 \phi_c\rangle = \frac{\int_0^{\pi/2}\int_0^{2\pi} I_c(\phi_c, \alpha)\cos^2\phi_c \sin\phi_c \, d\alpha \, d\phi_c}{\int_0^{\pi/2}\int_0^{2\pi} I_c(\phi_c, \alpha)\sin\phi_c \, d\alpha \, d\phi} \quad (2)$$

Linear coefficients of thermal expansion (CTE) of the fibres were measured by a Seiko Stress/Strain thermal mechanical analyser (TMA/SS 100). A single filament with a diameter ranging from 10 to 50 μm was clamped into the sample holder with different initial stresses applied. The changes of the fibre length (percentage of elongation) as well as the slopes of such changes with temperature (CTE) were recorded for fibres with different draw ratios. The heating rate was 10°C min^{-1} over a temperature region between 30°C and 500°C.

Thermal dynamic mechanical (DM) measurements were conducted on a Rheometrics solid state analyser (RSA II) in the temperature/frequency sweeping mode. Single filaments were again clamped into a sample holder where an initial strain ranged from 0.001% to 0.005%. Different initial strains were used, and little difference was found among the fibres' DM data. However, a relatively high strain level did help for obtaining data with low noise. The frequency applied was between 0.01 Hz and 10 Hz over a temperature range from 30°C to 500°C. Storage (E'), loss (E'') moduli were measured for fibres of different draw ratios. Also, the tan δ was calculated through E' and E''.

RESULTS AND DISCUSSION

Overall and crystal orientations

Figure 1 combines two different orientation parameters of the fibres with different draw ratios: overall orientation (birefringence Δn) measured from o.b. experiments; and crystal orientation along the (003) crystallographic plane measured from WAXD experiments. It is not surprising that, by increasing the draw ratio, both orientation parameters are increased. Nevertheless, the rates of change are different. The crystal orientation builds up relatively fast in the initial stage of the drawing process. For example, at a draw ratio of three, the crystal orientation factor along the (003) plane is 0.75, which is about 83% of the final crystal orientation (0.90) achieved in the fibres. At about a draw ratio of six times, this orientation factor reaches 0.85, and a further increase in the draw ratio does not significantly improve the crystal orientation. Only a minor increase in the crystal orientation factor can be observed up to about 0.88 at a draw ratio of eight. On the other hand, the overall orientation behaves differently. In the low draw ratio region the birefringence value increases almost parallel to the development of the crystal orientation factor.

However, at high draw ratios the birefringence value still increases. This indicates that at high draw ratios the main contribution to the overall orientation comes from the non-crystalline region in the fibres. Similar observations were reported in other synthetic fibres such as polyesters and polyamides[7–9].

Figure 2 illustrates a relationship between crystallinity and draw ratio of BPDA–PFMB fibres. It is evident that by increasing the draw ratio the crystallinity in the fibres increases from 10% at a draw ratio of one to 50% at a draw ratio of eight. However, this relationship is non-linear. The crystallinity develops quickly at the low draw ratios and gradually levels off at high draw ratios, which is in-between the behaviour of overall orientation and crystal orientation developments (*Figure 1*). In fact, the orientation in the fibres leads to the chain molecules parallel to each other, and provides precursors for further crystallization (orientation-induced crystallization). It should also be noted that tensile strength and modulus of the fibres increase continuously after a draw ratio of six times. This reveals an effect of orientation in the non-crystalline region to the mechanical properties.

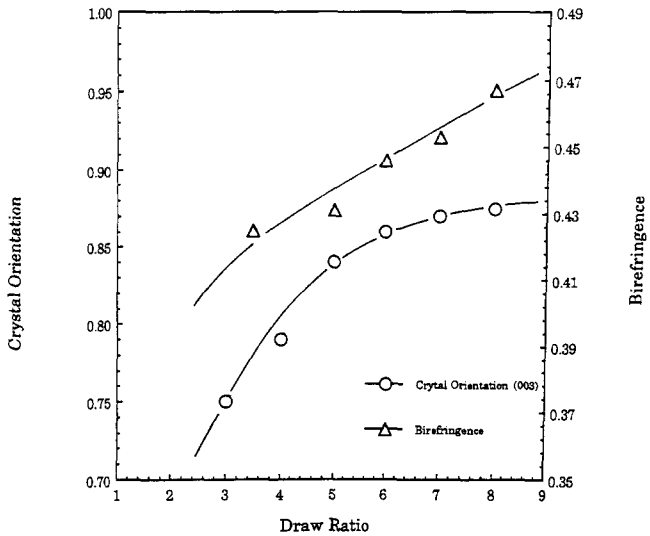

Figure 1 Relationships of overall and crystal orientations with draw ratio in BPDA–PFMB fibres

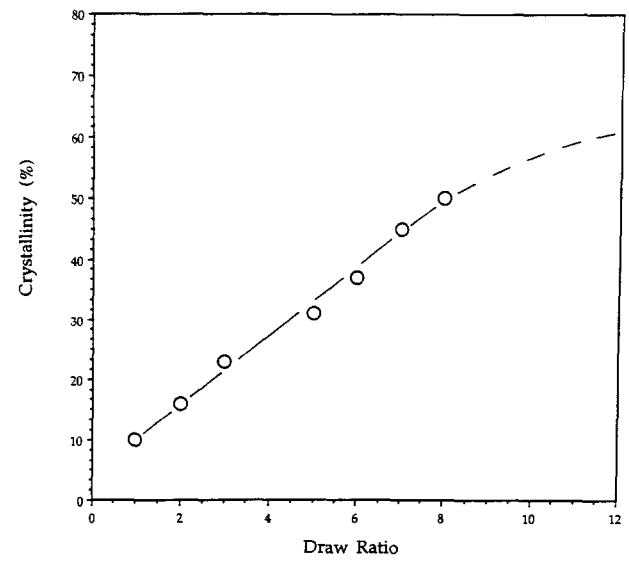

Figure 2 Relationship between crystallinity and draw ratio in BPDA–PFMB fibres

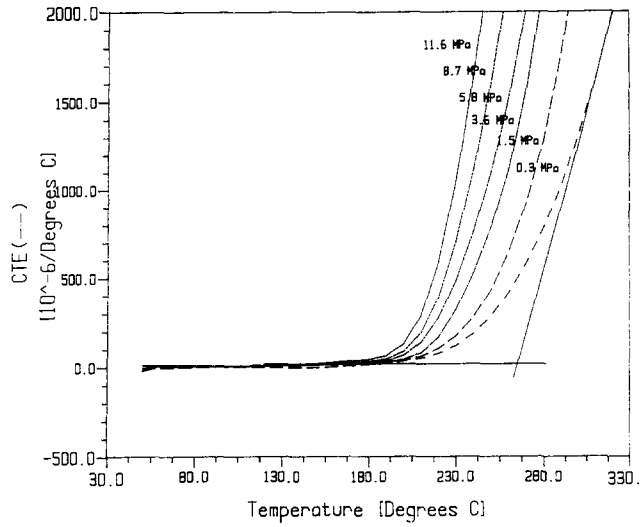

Figure 3 Coefficients of thermal expansion of the as-spun fibres at different temperatures and stresses applied

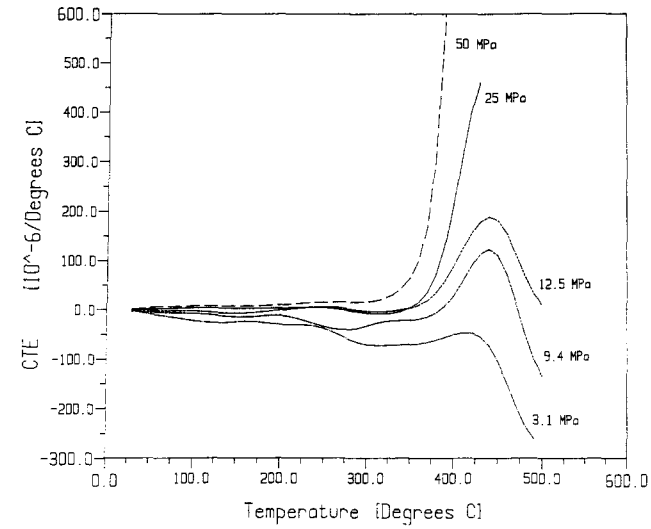

Figure 4 Coefficients of thermal expansion of the fibres with four times draw ratio at different temperatures and stresses applied

Linear coefficients of thermal expansion

Figure 3 shows relationships between CTE and temperature for as-spun fibres at different stresses applied during the TMA measurements. In the solid state the CTEs of fibres exhibit slightly negative values at low stresses (it is not obvious in the figure due to the large scale of the percentages of elongation). By increasing this stress, the CTEs move toward positive values. For example, the CTE between 50°C and 150°C for the as-spun fibres is $2.5 \times 10^{-6}\,°C^{-1}$ at a stress level of 0.5 MPa, and it increases to $5.0 \times 10^{-6}\,°C^{-1}$ at a stress level of 6 MPa. Furthermore, all the CTE data show a transition temperature where the CTE exhibits a drastic change. This is an indication of the glass transition temperature (T_g) of as-spun fibres (see below).

Figure 4 represents the CTE data for the fibres at a draw ratio of four times, as an example. Generally, a negative CTE in the solid state can be found at a low stress level, which gradually increases with applied stress. When the temperature rises, an increase of CTE (elongation) followed by a decrease of CTE (shrinkage) can be observed at low stress applied below 15 MPa in a temperature region of 350–500°C. The increase in CTE

becomes more dominant and shifts to lower temperatures with increasing the stress above 15 MPa. However, above this applied stress no decrease in CTE at high temperatures can be seen. Comparing with as-spun fibres, furthermore, the transition where the change of CTE is observed occurs at higher temperatures, and the change of absolute CTE values are also smaller. This indicates that by increasing the draw ratio (thus crystallinity) the glass transition shifts to higher temperatures and is less observable (see below).

Figure 5a shows that CTE values in solid state change with the stress applied for as-spun fibres. It is interesting that the CTE increases initially from a value which is lower than the CTE of in-plane oriented BPDA–PFMB films ($6.98 \times 10^{-6}\,°C^{-1}$)[10] when the stress applied is below about 6 MPa. Between the stress levels of 6 and 10 MPa the CTE plateaus at about $(5-8) \times 10^{-6}\,°C^{-1}$. Further increase in the stress applied leads to an increase in CTE again. The low CTEs exhibited at the low stress level are due to a small internal stress frozen into the fibre during the spinning process. When the stress applied is less than the internal stress, a low CTE is observed.

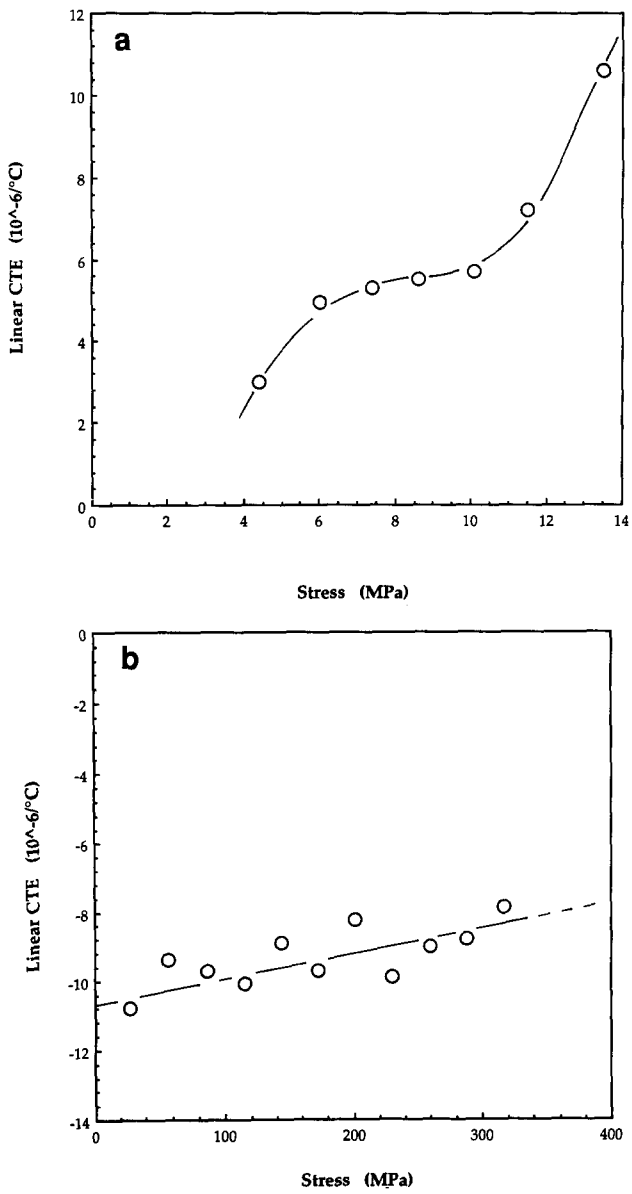

Figure 5 Relationship between the CTEs in the solid state of (a) the as-spun and (b) four times draw ratio fibres and stress applied

When the stress applied reaches a level which is close to the internal stress frozen into the fibre, a CTE close to that of in-plane oriented films can be found. At an even higher applied stress, a higher CTE is observed because the internal stress is overcome by the stress applied. Experimental results observed for the fibres with a draw ratio of four (*Figure 5b*), however, show that the initial CTE in this case is much more negative compared with those in as-spun fibres. Moreover, the stress applied up to 300 MPa only reaches a CTE of $-8.5 \times 10^{-6}\,°C^{-1}$. This indicates that one needs a much higher stress applied to balance the internal stress. Namely, a draw ratio of four has introduced an internal stress frozen into the fibres which must be about several orders of magnitude higher than that in as-spun fibres. This observation can, in turn, be used to explain the CTE behaviour shown in *Figure 4*. A detailed study of the internal stress frozen into the fibres during drawing is under investigation.

Furthermore, from a microscopic point of view, the internal stress frozen in during the drawing can be attributed to two processes: an elastic deformation of bond lengths and bond angles; and a plastic deformation. These behaviours are expected since BPDA–PFMB molecules are relatively rigid, and the *trans* conformation of the molecules is a major population in the highly drawn fibres. A simple series model[11] is perhaps enough to describe the fibre structure. Moreover, the crystallinity of the fibres can be as high as about 50%[1]. It is highly possible that the frozen-in stress may be distributed in both crystalline and oriented non-crystalline regions. A release of this stress at high temperatures observed through the CTE measurements in TMA experiments should be largely attributed to the relaxation of the stress from the non-crystalline region. This judgement is based on the fact that one cannot observe the crystal melting in the fibres below the decomposition temperature (600°C)[12]. For the as-spun fibres, the crystallinity is very low (less than 10%), and the stress frozen into the fibres is also low. This leads to a relatively large change of the CTE at T_g.

Glass transition temperatures

Figure 6 illustrates the relationship between T_g and stress applied for the as-spun fibres, where the T_g is defined to be the onset temperature of the change in CTEs observed in *Figure 3*. It is shown that a linear function between T_g and applied stress (σ) exists with a negative slope in the low stress region of below about 6 MPa. When one extrapolates the T_g to $\sigma = 0$, a T_g° can be obtained for as-spun fibres, which is approximately 290°C. This can be compared with the glass transition temperature of 287°C obtained by a similar extrapolation method for in-plane oriented BPDA–PFMB films[10]. The slope indicates how sensitive the T_g change is to the stress applied. In this stress region the slope in *Figure 6* is also close to that extrapolated from in-plane oriented BPDA–PFMB films[10]. However, at higher applied stresses during measurements a positive deviation toward a higher T_g can be observed. This phenomenon actually reveals by increasing the applied stress, it induces orientation, and therefore crystallization as long as the molecules have a chance to move. As a result, the sensitivity to the stress applied reduces due to the fact that the stress applied frozen into the crystalline region of the fibres cannot now be released in this temperature range. A quantitative treatment of the glass transition

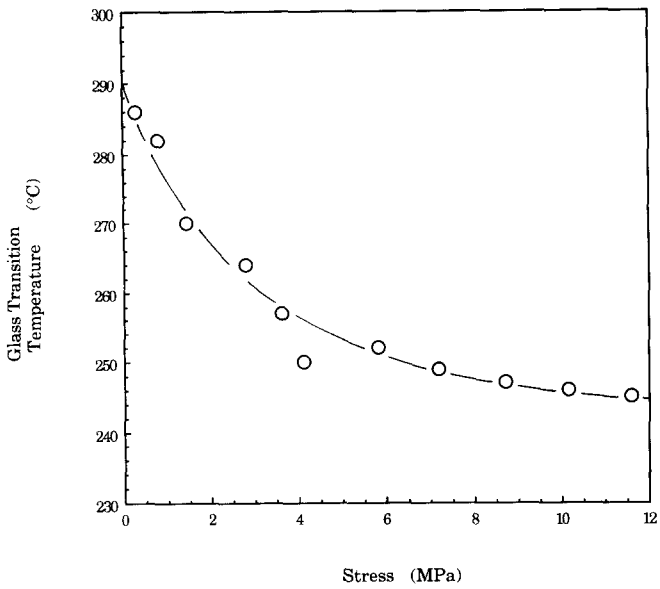

Figure 6 Relationship betwen T_g of the as-spun fibres and initial stress applied

temperature with stress applied was proposed by Chow several years ago[13–15]. A relationship between T_g and stress applied ($\sum$) can be expressed as

$$T_g = T_g^\circ + [RT_r^2/(\varepsilon)]\{1 - \exp[V\sum/(RT)]\} \quad (3)$$

where ε is the average energy of hole formation, T_r is a reference temperature, V is the tensile-activation volume and R is the universal gas constant. Equation (3) was originally adopted for the case of unoriented samples under different stress applied at negligible strain rate. To use this equation in the oriented fibres, the stress term ($\sum$) here must be understood as a summation of the applied stress and the internal stress frozen in (note that they possess opposite signs). If $V\sum$ is small and approaches zero, equation (3) becomes

$$T_g \sim T_g^\circ - T_r V\sum/\varepsilon = T_g^\circ - k\sum \quad (4)$$

where k has a unit of °C MPa^{-1}. It should be noted that in *Figure 6* the horizontal axis is applied stress, but not $\sum$. Under the assumption that the internal stress frozen in is a constant and small in the low stress level applied (say, below 6 MPa), the plot can still be representative of the relationship described by equation (4).

On the other hand, increasing the draw ratio causes the glass transition to vanish quickly due to the increase in orientation and crystallinity. For example, at a draw ratio of about two times, the glass transition temperature measured from TMA can only be barely observed. The effect of the orientation and crystallinity on glass transition will be discussed in the next section.

Dynamic mechanical behaviour

Figure 7 shows experimental DM data (E', E'' and tan δ) for as-spun fibres at four different frequencies (0.01, 0.1, 1 and 10 Hz). It is obvious that two relaxation processes can be identified above room temperature: an α relaxation which corresponds to the glass transition and a β relaxation which is a subglass transition. The peak temperature of the β relaxation is more sensitive to the frequency compared to that of the α relaxation. Furthermore, the magnitude in tan δ of the β relaxation is between 0.3 and 0.4, while that of the α relaxation is about 0.3–0.9, depending upon the frequency measured. Interestingly enough, the magnitude of tan δ is unusually large at low frequency due to a substantially low E'. This may be an indication that a low-frequency motion is involved in the β relaxation process.

When one conducts DM experiments on the drawn fibres, as shown in *Figures 8a* and *8b* (a draw ratio of four and six times, respectively), it is interesting to find that first, the sensitivity to the frequency of the β relaxation peak decreases, and its magnitude in tan δ is also clearly reduced to 0.08–0.2. If one extrapolates this

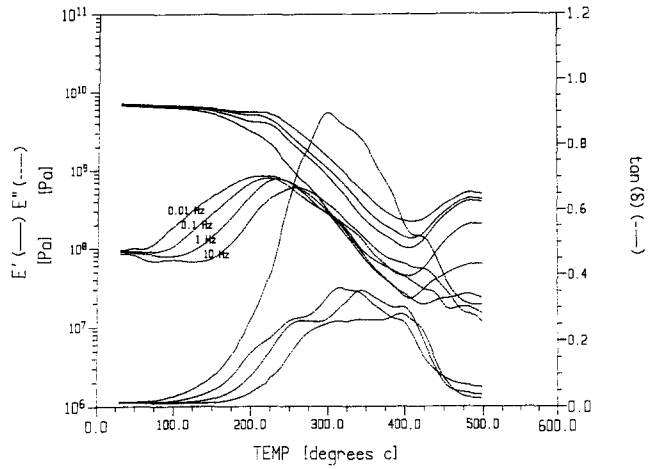

Figure 7 Dynamic mechanical data of the as-spun fibres at different frequencies

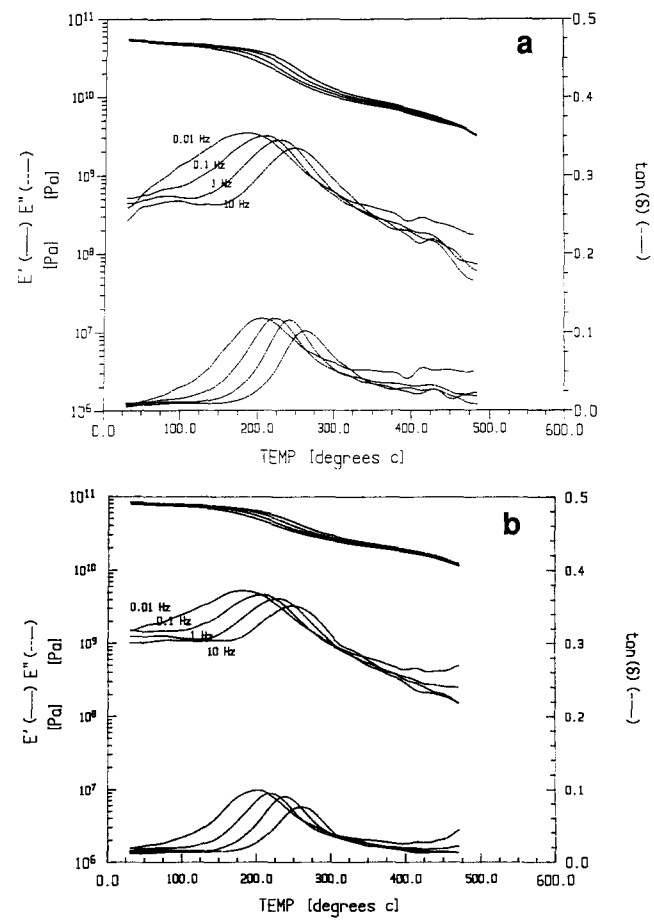

Figure 8 Dynamic mechanical data of the fibres (a) with four times draw ratio and (b) with six times draw ratio at different frequencies

magnitude of the β relaxation peak to 100% crystallinity, this magnitude is very close to zero, as shown in *Figure 9*. This indicates that the β relaxation process is crystallinity dependent in the fibres. An active discussion of the origin of the β relaxation process in aromatic polyimides has been undertaken over many years[16–22]. Recently, we have found that this β relaxation process is associated with non-cooperative motion of uncrystallized diamines in many aromatic polyimide films[23]. In this case, therefore, the β relaxation process should be attributed to uncrystallized PFMB diamines.

A very interesting observation is the α relaxation process. At a draw ratio of four and six times, the crystallinities of 27% and 38% can be achieved in the fibres, respectively. However, from *Figures 8a* and *8b* the α relaxation process is almost totally suppressed. It should be noted that a glass transition must correspond to segmental motion which is attributed to a mobile amorphous region of polymer materials. This shows that the segmental motion in the non-crystallized region of the fibres, which is as high as 70% of the total fibre material, is suppressed due to the presence of the crystallinity and internal stress frozen into the fibre. This portion of the material is thus still rigid above its glass transition. It is similar to the concept of rigid amorphous fraction proposed several years ago[24,25]. The difference is that this material is highly oriented. On one occasion we have also found that the rigid amorphous fraction shows its correspondence with oriented amorphous material in uniaxially drawn poly(ethylene-2,6-naphthalene dicarboxylate) films[26]. Therefore one can conclude that the α relaxation is more precisely rigid fraction dependent.

Turning to the Arrhenius activation energy of the β relaxation process, one can plot a relationship between logarithmic frequency and the reciprocal of the peak temperature for the loss modulus. For as-spun fibres, this relationship is shown in *Figure 10*. The activation energy E_a calculation from its slope is 160 kJ mol^{-1}, which is slightly higher than the value obtained from unoriented BPDA–PFMB films (130 kJ mol^{-1})[10]. As has been discussed elsewhere[23,27], the value of $E_a = 130$ kJ mol^{-1} indicates a largely non-cooperative motion based on the Erying absolute rate approach suggested by Starkweather[28]. As-spun fibres have some degree of orientation introduced during the spinning process, and therefore a certain cooperativity of the motion may be introduced. For drawn fibres above the draw ratio of 1.5 it is clear that the activation energy rises. Moreover, it seems that the activation energy is draw ratio independent, and shows a constant of around 210 kJ mol^{-1} as shown in *Figure 10*. An increase of about 50 kJ mol^{-1} illustrates that the motion of the PFMB moiety in the oriented fibres is more cooperative in nature. A draw ratio independence of the activation energy may be an indication of a saturation of the non-cooperative PFMB motion in drawn fibres. This may be explained by an increase in molecular packing density and crystallinity in the oriented fibres. It is also possible to calculate the apparent activation energy using the same relationship to the α relaxation process for as-spun fibres, which is about 800 kJ mol^{-1} in a narrow frequency range (0.001–10 Hz). It should be pointed out, however, that in a wide frequency range this relationship must be no longer linear and fit to a WLF equation[15].

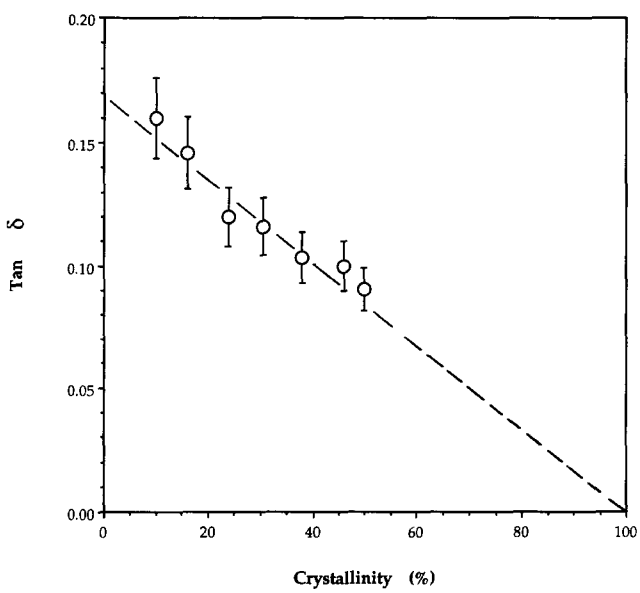

Figure 9 Relationship between the intensity of β relaxation and crystallinity in the fibres

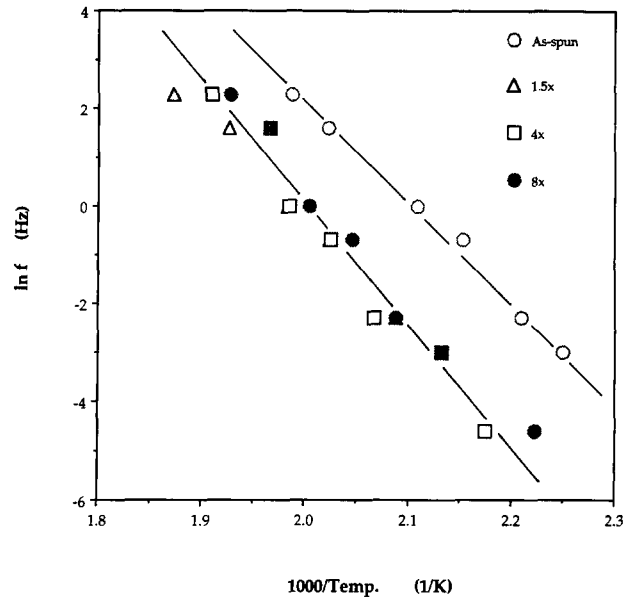

Figure 10 Relationship between logarithmic frequency and reciprocal peak temperatures of the β relaxation in as-spun fibres and fibres with different draw ratios

Finally, it should be noted that the value of E' shown in *Figures 7*, *8a* and *8b* increases from about 7 GPa for the as-spun fibres to 90 GPa for the fibres with a draw ratio of six times. Further increasing the draw ratio in the fibres leads to a E' value of 130 GPa as reported in reference 1.

CONCLUSION

We have reported that BPDA–PFMB fibres show increasing overall and crystal orientations with increasing the draw ratio. At high draw ratios the overall orientation increase is mainly due to the contribution of the non-crystalline region in the fibres. At low applied stress levels linear CTEs of the fibres are negative and decrease with increasing the draw ratio. This is due to the internal stress frozen in during the fibre-drawing process at elevated temperatures. However, for each different draw

ratio there is a different stress region where the CTE is close to $(5-8)\times10^{-6}\,°C^{-1}$ (close to the CTE of in-plane oriented films). This reveals that in this stress region for each fibre the internal stress frozen in during the drawing process is roughly equal to the stress applied. Further increasing the stress leads to an increase in the CTEs. Dynamic mechanical measurements indicate that two relaxation processes exist above the room temperature: α and β transitions. The α transition corresponds to the glass transition with an apparent activation energy of around $800\,kJ\,mol^{-1}$, while the β transition is a subglass transition with an activation energy of about $160\,kJ\,mol^{-1}$ for as-spun fibres. This β transition is associated with some degree of non-cooperative motion in the non-crystalline PFMB of the fibres and is therefore crystallinity dependent. By increasing the draw ratio above 1.5, the non-cooperativity is lost due to the orientation and crystallization of the chain molecules, evidenced by a $50\,kJ\,mol^{-1}$ increase in the activation energy ($210\,kJ\,mol^{-1}$).

ACKNOWLEDGEMENTS

This work was supported by NSF/Ohio/Industry Center for Molecular and Microstructure Composites (CMMC) at The University of Akron and Case Western Reserve University and SZDC's Presidential Young Investigator Award (DMR-91-57738) and industrial matching funding provided by Hercules Inc.

REFERENCES

1 Cheng, S. Z. D., Wu, Z. Q., Eashoo, M., Hsu, S. L.-C. and Harris, F. W. *Polymer* 1991, **32**, 1803
2 Harris, F. W. in 'Polyimides' (Eds D. Wilson, H. D. Stenzenberger and P. M. Hergenrother), Chapman and Hall, New York, 1989, pp. 1–37
3 Harris, H. W. and Hsu, S. L.-C. *High Perform. Polym.* 1990, **1**, 3
4 Lee, S. K., Lee, C. J., Harris, F. W. and Cheng, S. Z. D. *Polym. Int.* 1993, **30**, 115
5 Cheng, S. Z. D., Arnold, F. E. Jr, Hsu, S. L.-C. and Harris, F. W. *Macromolecules* 1991, **24**, 5856
6 Hamza, A. A. and El-Kader, N. I. *Textile Res. J.* 1983, **53**, 205
7 Balcerzyk, E., Kozkowski, W., Wesol'owska, E. and Lemnszkiewicz, W. *J. Appl. Polym. Sci.* 1981, **26**, 2573
8 Long, S. D. and Ward, I. M. *J. Appl. Polym. Sci.* 1991, **42**, 1911
9 Rim, P. B. and Nelson, C. J. *J. Appl. Polym. Sci.* 1991, **42**, 1807
10 Arnold, F. E. Jr, Shen, D.-X., Lee, C. J., Cheng, S. Z. D. and Lau, S.-F. *Polymer* 1992, **33**, 5179
11 Wu, Z.-Q., Zhang, A.-Q., Cheng, S. Z. D., Huang, B. and Qian, B.-J. *J. Polym. Sci., Polym. Phys. Edn* 1990, **28**, 2565
12 Eashoo, M. PhD dissertation, Department of Polymer Science, The University of Akron, Akron, Ohio, 1994
13 Chow, T. S. *Polym. Eng. Sci.* 1984, **24**, 915
14 Chow, T. S. *Polym. Eng. Sci.* 1984, **24**, 1079
15 Chow, T. S. *J. Polym. Sci., Polym. Phys. Edn* 1987, **25**, 137
16 Ikeda, R. M. *J. Polym. Sci., Polym. Lett. Edn* 1966, **4**, 353
17 Bemier, G. A. and Kline, D. E. *J. Appl. Polym. Sci.* 1968, **12**, 593
18 Perena, J. M. *Makromol. Chem.* 1982, **106**, 61
19 Butta, E., de Pefris, S. and Pasquoni, M. *J. Appl. Polym. Sci.* 1969, **13**, 1073
20 Mitchenko, Yu. I., Dolgov, A. V. and Krasnov, E. P. *Vysokomol. Suedin.* 1975, **A17**, 2091
21 Krasnov, E. P., Stepan'yan, A. E., Mitchenko, Yu. I., Tolkachev, Yu. A. and Lukasheva, V. N. *Vysokomol. Suedin.* 1977, **A19**, 1566
22 Bessonov, M. I., Koton, M. M., Kudryavtsev, V. V. and Lains, V. V. 'Polyimides, Thermally Stable Polymers', Consult. Bureau, New York, 1987, pp. 250–251
23 Arnold, F. E. Jr, Bruno, K., Eashoo, M., Lee, C. J., Harris, F. W. and Cheng, S. Z. D. *Polym. Eng. Sci.* (in press)
24 Susuki, H. and Wunderlich, B. *Br. Polym. J.* 1985, **17**, 1
25 Cheng, S. Z. D. *J. Appl. Polym. Sci.* 1989, **43**, 315
26 Cheng, S. Z. D., Janimak, J. J., Zhang, A.-Q. and Chu, A.-L. *Polym. Bull.* 1988, **20**, 449
27 Arnold, F. E. Jr., Shen, D.-X., Lee, C. J., Harris, F. W. and Cheng, S. Z. D. *J. Mater. Chem.* 1993, **3**, 189
28 Starkweather, H. W. Jr *Polymer* 1991, **32**, 2443